Investigating the Effect of Various Augmentations on the Input Data Fed to a Convolutional Neural Network for the Task of Mammographic Mass Classification

Conference Paper *in* Communications in Computer and Information Science · June 2017

DOI: 10.1007/978-3-319-60964-5_35

CITATIONS
7

READS
114

4 authors:

Azam Hamidinekoo
Institute of Cancer Research
12 PUBLICATIONS **54** CITATIONS
SEE PROFILE

Zobia Suhail
University of the Punjab
13 PUBLICATIONS **38** CITATIONS
SEE PROFILE

Talha Qaiser
The University of Warwick
19 PUBLICATIONS **452** CITATIONS
SEE PROFILE

Reyer Zwiggelaar
Aberystwyth University
264 PUBLICATIONS **2,739** CITATIONS
SEE PROFILE

Investigating the effect of various augmentations on the input data fed to a Convolutional Neural Network for the task of mammographic mass classification

Azam Hamidinekoo[1], Zobia Suhail[1], Talha Qaiser[2], and Reyer Zwiggelaar[1]

[1] Department of Computer Science, Aberystwyth University
[2] Department of Computer Science, Warwick University

Abstract. Along with the recent improvement in medical image analysis, exploring deep learning based approaches in the context of mammography image processing has become more realistic. In this paper, we concatenate on both conventional machine learning and deep learning approaches to classify mass abnormalities in mammographic images. Using a deep convolutional neural network (CNN) architecture, the effect of performing various augmentation approaches on the raw pre-detected masses fed to the network is investigated. We propose an extended augmentation method, specific filter bank responses and also a texton-based approach to generate characteristic filtered features for various types of mass textures and eventually use the resulting image data as input for training the CNN. Evaluating our proposed techniques on the DDSM dataset, we show that mammographic mass classification can be tackled effectively by employing an extended augmentation scheme. We obtained 87% accuracy which is comparable to the currently reported results for this task.

Keywords: breast cancer, mammographic mass classification, data augmentation, Convolutional Neural Network (CNN)

1 Introduction

Breast cancer is the most frequently diagnosed type of cancer worldwide [2] which accounts for 25.2% of the total cancer related death among women followed by colorectum (9.2%), lung (8.7%), cervix (7.9%), and stomach cancers (4.8%) according to the report by International Agency for Research on Cancer, WHO in 2014 [26]. The assessment process for breast screening is based on a imaging for finding early changes in breast tissue, plus clinical assessment and needle biopsy if required [1]. Mammography scans (mammograms) are used as a primary imaging modality to identify the abnormalities at early stages. Moreover, two main appearances shown in mammograms are masses and microcalcifications [6]; and Computer Aided Diagnosis (CAD) systems have been developed for each. However, the variability among different masses with respect to shape and boundary causes misdiagnosis of masses in mammographic images.

Up to now, various conventional machine learning methods and deep learning approaches have been explored for the task of breast mass classification and diagnosis which will be covered in the next section. In this paper, we try to concatenate both conventional and deep learning approaches to classify benign and malignant breast masses. So the main aim of this paper is to classify mammographic masses using a deep convolutional neural network (CNN) architecture and investigate the effect of performing data augmentation on the raw pre-detected masses fed to the network. For this aim, 3 different new augmentation schemes are proposed and the results are evaluated on a public dataset.

2 Related Work

Various conventional machine learning methods for the task of mammographic mass classification are reviewed in [20]. Moreover, a three steps procedure for the classification of benign and malignant masses is proposed in [25] in which the RoI segmentation is done with a group of 32 Zernike moments that were extracted to train a neural network. Vaidehi *et al.* [28] proposed a method using Gray Level Co-occurrence Matrix (GLCM) features including contrast, correlation, energy and homogeneity accompanied with the Fuzzy C-Mean technique to extract GLCM features for mass classification. Buciu *et al.* [4] proposed directional features extracted by filtering image patches using Gabor wavelets. Reducing the data dimension by Principal Component Analysis (PCA), they improved classification results when Gabor features are used instead of using original mammogram images. Additionally, texton-based approaches have been used effectively for the texture classification using single images [30], where the textures are represented as histograms of texton contained in texton dictionary. In a similar work, Varma *et al.* used filter responses in order to build texton dictionary. They demonstrated that such textures could be classified using joint distribution of intensity values [29]. However, these methods- considered as the conventional methods- rely on hand designed feature extractors that require a considerable amount of engineering skill and domain expertise. In recent years, the hand-crafted feature extraction aspect is proposed to be replaced by trainable deep networks which are able to extract discriminant features automatically from the images.

Considering the layer aspect of deep networks along with parallelisable algorithms and the vast acceleration property of GPUs, exploring deep learning based approaches in the context of mammography image processing has also become more realistic. Accordingly, Petersen *et al.* [21] presented a generic multi-scale denoising autoencoder for contextual breast density segmentation. Kallenberg *et al.* [16] tested a convolutional sparse autoencoder network with a sparsity regularisation on their own unlabelled sets of mammograms expanding the idea of [23] but for pixel-wise labelling and for large scale images. Jamieson *et al.* [13] explored the use of Adaptive Deconvolutional Networks for learning high-level features of mass lesions. Arevalo *et al.* [3] presented various depth CNN frameworks for automatic supervised feature learning of film mammograms. Fonseca

et al. [9] evaluated the performance of an architecture search procedure [22] and Dhungel *et al.* [8] presented a multi-scale deep belief network combined with a Gaussian Mixture Model classifier for mass candidate generation. Kooi *et al.* [17] and Huynh *et al.* [12] took advantage of transfer learning to extract tumour information from medical images via CNNs that were originally pre-trained with non-medical data. In a similar way, Jiao *et al.* [15] used a pre-trained CNN on LSVRC images [7] and fine-tuned on a subset of breast mass images.

Deep learning is becoming a powerful tool for image classification. In medical imaging the lack of images/ examples has been described as the main drawback for their development [10]. Considering the use of deep learning methods to address breast mass classification, deep networks are also difficult to train from scratch for breast mass images because of the small number of samples and the existing variance in various mammographic appearances which makes it difficult to combine all available images. Transfer learning and data augmentation have been proposed as promising solutions for overcoming such lack of data [18, 27]. As new solutions for this issue in the mammographic mass classification problem, in this study, firstly, data augmentation as was suggested in [18] is extended conceptually to acquire more data to train a deep CNN architecture. In another experiments, two texture discovery techniques are proposed to generate informative mass pattern representations to alleviate the value of train data.

3 Dataset

The benchmark dataset used in our experiments is publicly available Digital Database for Screening Mammography (DDSM) [11] which is a wide ranging annotated film mammography based repository provided by the University of South Florida. DDSM provides nearly 2620 studies of both mediolateral oblique (MLO) and cranio caudal (CC) views of each breast accompanied by a mask if an abnormality is present. The images are grey-level mammograms with the bit depth of 16 bits per pixel.

Using the annotated mass lesions, first of all, 947 cases were selected after manually removing distorted images for our designed experiments. Eventually a subset of 990 and 943 images containing annotated regions of interests (RoIs) were used identifying benign and malignant lesions respectively. The women cases were randomly split into train, validation and test sets by 80%, 10% and 10% of the whole database respectively. Using the approach proposed in [19], we extracted two patch forms (bounding box and double bounding box) from the annotated images and used them as input patches for further procedures described in section 4.1.

In the first and the second experiment, we performed augmentation on the selected train dataset which contained 367 benign cases and 352 malignant cases. In the third experiment, we considered a subset of 400 cases, comprising 200 benign and 200 malignant cases. These cases were randomly selected from the whole women in dataset dedicated for training. Using the annotated RoI, a bounding box of the mass was extracted and subsequently resized into 224×224

pixels to be used as an input patch for further processing that will be explained more in details in section 4.3.

4 Train data augmentation scheme

One of the aims of this study is to compare the effect of performing image preprocessing on the raw extracted patches. Thus, we performed three separate experiments. In the first experiment we used raw image patches with augmentation as the input training data for the deep network. In the second experiments, we used specific filter bank responses from the extracted RoIs. In the third experiment, we used a texton-based approach to generate characteristic features for various types of mass textures and eventually used the resulted textons as the input data for training a convolutional neural network.

4.1 Experiment I

Inspired by [19] and [18], one approach to alleviate the constraint size of training is to consider the area surrounding the bounding box of an annotated mass. Therefore, two different patch contexts from the training images were selected without implementing any variations in the image intensity. However, data augmentation was performed to compensate for the small amount of data. So, as shown explicitly in Figure 1, original images, selected for training, are randomly rotated by angles in the $0 < \theta < 360$ range and the following patch contexts are extracted from each rotated image:

1. Bounding box of the annotated mass: (BB)
2. Two times the bounding box (double bounding box) of the annotated mass: (D-BB)

The resulting black corners from the rotation were filled with the mean pixel value of that image in order to avoid significant distortion for the abnormalities that are located near the image borders. In the next step, each patch is resized to 224 along the shorter side and then five random crops are performed on each rotated and extracted context. Finally, mirroring was done resulting in totally 50 augmented images for each training example beside its original sample. The idea behind this augmentation is that not only masses can have different orientations but also the mass neighbourhood may have relevant informative values. Therefore, by these transformations, we were able to generate new labelled samples for a supervised mass lesion classification. This data augmentation scheme is depicted in Figure 1.

4.2 Experiment II

In the second experiment, the bounding box of the annotated masses were extracted and resized to 224×224. Samples of malignant and benign mammogram patches used in this experiment are shown in Figure 2. Inspired by the texton-

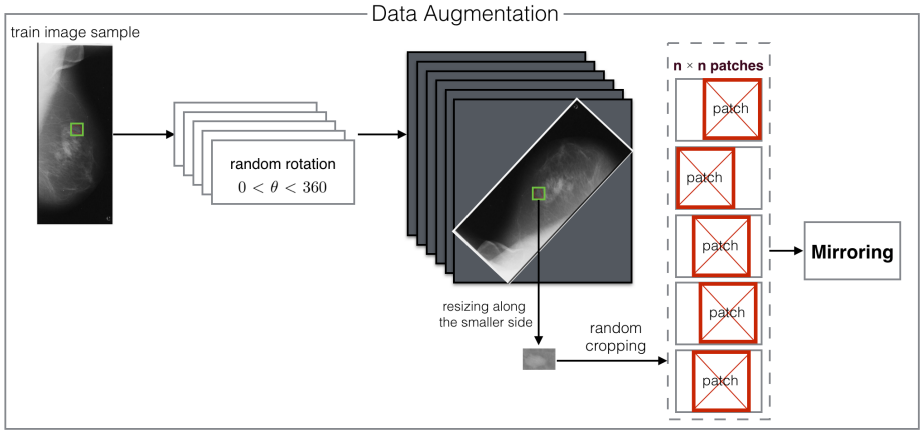

Fig. 1. Data augmentation scheme in experiment I resulting in $5 \times 5 \times 2$ augmented samples.

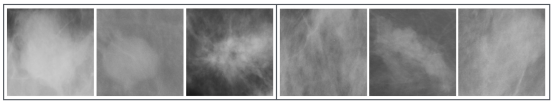

Fig. 2. Samples of malignant (3 left examples) and benign (3 right examples) mammogram patches from DDSM database.

based methodology proposed for the texture classification [30, 29], a texture-based and a texton-based approach using statistical distribution filter responses are used to prepare the input data for the deep network. To achieve this, firstly, we have selected a combination of 53 filters from the proposed Maximum Response (MR) and Schmid (S) filter banks [30] which are depicted in Figure 3. The first 38 filters are obtained from the MR8 filter bank and are a mixture of edge and bar filters at six orientations and three scales, a Gaussian and a Laplacian of Gaussian filters. The other 13 filters are obtained from the S filter bank which consists of various isotropic Gabor-like filters.

Using the selected filter bank, in the second experiment, the training database was convolved with the mentioned filters to generate filter responses. These responses actually extract various textural information from the RoI images and are possible candidates to be used in the augmented train set. The resulted responses for one RoI example from the train set is presented in Figure 4.

4.3 Experiment III

Subsequently, all the filter responses from the second experiment are normalised to zero mean and unit variance to put them in the same range. After getting filter

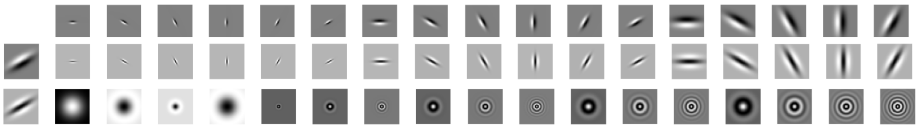

Fig. 3. Combination of MR and S filter banks used to make filter responses for generating a RoI-texton-model in experiment II.

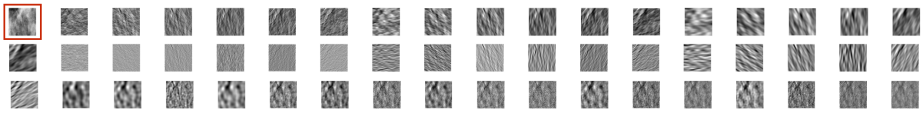

Fig. 4. Filter bank responses on one sample extracted RoI image that is shown in the red box.

responses for the selected train dataset, K-mean clustering is performed to define 15 clusters (textons) for each class. The reason to select 15 textons is related to the balance between accuracy and memory requirements. The higher the texton numbers, the higher the precision but at the same time memory requirements will increase.

Aggregating the textons from both classes, a texton dictionary is formed that composes 30 textons. The detailed steps involved in creating textons for each class can be found explicitly in Figure 5. Afterwards, each filter response from a RoI is assigned to the closest texton from the texton dictionary. Summing up the assigned textons, a new image is generated which we call a RoI-texton-model. Eventually, these created RoI-texton-models for each image are fed into the deep network as augmented samples. No cropping, rotation or mirroring is performed on these texton maps since it can change the inherent information stored in each RoI-texton-model related to a raw sample from a specific class.

The characteristics of the selected filters are: rotationally invariant, isotropic and anisotropic, multi-scale and multiple orientations which make the filters capable of generating good features for various types of mass textures. Thus, the idea behind the last two methodologies is that each filter in the filter bank reveals specific statistical information from the extracted RoIs which is addressed in the filter responses. Subsequently, created clusters of filter response distributions are expected to be mutual representative of a specific class. Additionally, due to the inherent characteristics of benign and malignant abnormalities, the generated clusters or textons in the texton dictionary for each class can be sufficiently discriminative to express the patterns hidden in a benign or a malignant lesion.

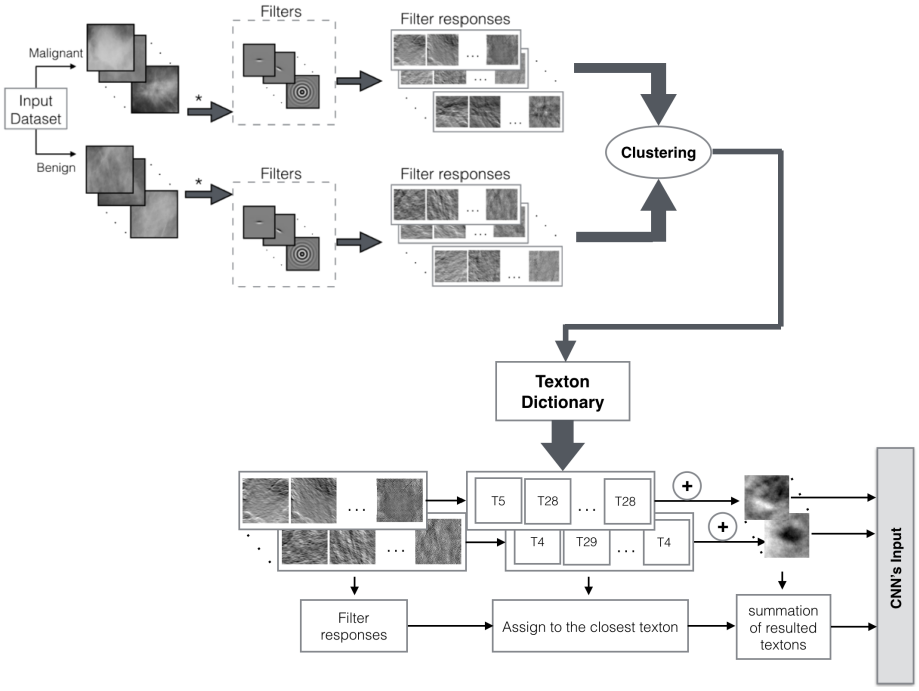

Fig. 5. Process of generating a texton dictionary and RoI-texton-models to augment the training data for CNN.

5 CNN architecture

The first work that popularised Convolutional Networks in Computer Vision was AlexNet, developed by Krizhevsky *et al.* [18] which was submitted to the ImageNet ILSVRC challenge in 2012 and significantly outperformed the runner-up. The Network has a deep architecture with five featured Convolutional Layers stacked on top of each other followed by pooling and finally three fully connected layers. In this work, we have used the same original architecture in all our experiments. Moreover, the last fully connected layer was changed into 2 outputs representing benign and malignant classes.

On the other hand, transfer learning is a machine learning technique, where knowledge gained during training on one type of problem is used to train on another similar type of problem. Tajbakhsh *et al.* [27] investigated the performance of deep CNNs trained from scratch compared with the pre-trained CNNs fine-tuned in a layer-wise manner. They tested various medical imaging applications from different imaging modalities and consistently showed that the use of a pre-trained CNN with adequate fine-tuning outperformed or, in the worst case, performed as well as a CNN trained from scratch. Some other studies [19, 12, 17, 7] have also confirmed the effectiveness of transfer learning. Ac-

cordingly, in this study, we initialised the AlexNet with pre-trained weights on the ImageNet dataset [24] (which consists of 1000 classes of images and 1.2 million training images) and fine-tuned it on our specific augmented training dataset. Using the same knowledge of ImageNet dataset features, the network is expected to identify mass abnormalities with less samples and training time. For this aim, convolutional layers are initialised with the pre-trained weights to identify features of the problem while the fully connected layers are removed from the trained network and retrained with fresh layers by a Gaussian distribution for our target classification task. Table 1 gives the specific parameter values we used during training AlexNet in our experiments. We also performed mean image subtraction during training the network. All classification implementations are performed within the Caffe framework [14] and the pre-trained model weights from the Caffe library and the visualisation facility of NVIDIA-DIGITS [3] are also utilised. Moreover, the computations were carried out using a NVIDIA GeForce GTX 1080 GPU on Intel Core i7-4790 Processor with Ubuntu 16.04 operating system.

Table 1. AlexNet parameter information.

optimisation scheme	SGD
base learning rate	0.001
learning policy	step-down
weight decay	0.005
momentum	0.9
dropout rate	0.5
epochs	30
train batch size	128
validation batch size	64

6 Results and Discussion

Using the pre-trained AlexNet model with the mentioned parameter values and fine-tuning on augmented training data from experiment I (AUG-1) and using the unseen test dataset, classification results of a deep network trained on two extracted context sizes are reported in Table 2. First of all, selecting a larger bounding box (double size) around the annotated mass to achieve higher classification accuracy (Acc: 81%) is confirmed since neighbouring context of the abnormality contains useful information which adds to the value of the samples considered in training data.

Moreover, adding the filter responses to the augmented data from experiment I, increased the accuracy result of the classification (85.19%) which we show with AUG-2. To understand why such accuracy is achieved, we should understand how

[3] https://developer.nvidia.com/digits

the network manages to achieve mass classification ability in both experiments. In AlexNet, the most interpretable convolution layer is filters in the first layer which are shown in Figure 6. These filters can capture horizontal, vertical and

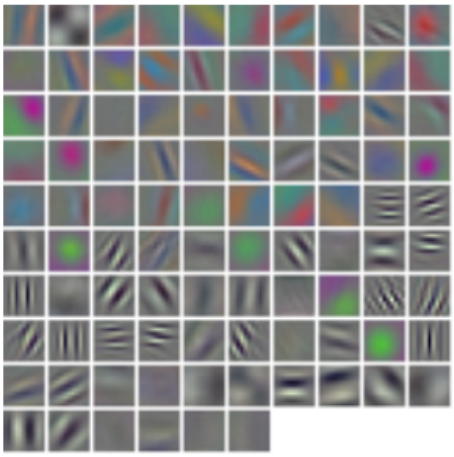

Fig. 6. Generated filters of the first convolutional layer in AlexNet.

parallel edges. Moreover, some of them have diagonal orientations and some look for high frequencies. This filter bank is applied to the input image and the maximum response from each 11×11 block is taken by pooling, giving these filter responses to the next layer. These are the low level features that are extracted from the input images. However, the filter responses from our suggested filter bank, in experiment II, are applied on the whole extracted RoI. These filters are proved to extract the most significant features from texture patterns [30]. Furthermore, some of these filters are not included in the first layer of the CNN which trys to captures low level features. So, the idea was to impose such filter responses to the network and we did it one time with bounding box contexts and another time by double bounding box contexts. The results showed better results while using filter responses from bounding box around the RoIs (85.8% using the bounding box compared to 85.1% using responses from double the bounding box around the RoIs). The reason can be interpreted as a possible zooming behaviour that can happen while using a bounding box context among double the bounding box extracted samples which eventually helped to the learning procedure.

On the other side, while making a RoI-texton-model of some random train samples, clusters of salient textural patterns for each class capture the relevant information related to one specific class and presents such textural characteristics in the resulted RoI-texton-model. The more textons selected from one class, the more common behaviour of that class is recorded in the RoI-texton-model. Considering this effect and adding this augmentation on a subset of training data

to the previously augmented data, eventually the trained network can extracts more discriminative features for classification and obtaining 87% accuracy.

Comparing the results reported in the confusion matrix, TP rate representing the number of true classified malignant masses are significantly improved and FN rate representing the number of misclassified malignant cases as benign cases are decreased which is very crucial in developing CAD systems. Beside these improvements, by increasing the number of TN which represents the number of true classified benign cases the need for further biopsy as an invasive procedure can be avoided.

Table 2. Classification results using various augmentations. (BB: bounding box of the training RoI image, D-BB: double bounding box of the training RoI image; AUG-1/2/3 represent augmentation method explained in experiments I, II and III respectively)

Type of training data	TN	FP	FN	TP	**Acc**
AUG-1 on BB	53	12	48	49	62.96%
AUG-1 on D-BB	73	13	17	59	81.48%
AUG-1 & AUG-2 on D-BB	71	15	9	67	85.19%
AUG-1 on D-BB & AUG-2 on BB	72	14	9	67	85.8%
AUG-1 on D-BB, AUG-2 & AUG-3 on BB	76	10	11	65	87.04%

Comparing classification results with the competing methods, it is comparable to the current approach outcomes [19, 5]. However, using different number of images in DDSM dataset and various evaluation metrics does not make a fair comparison. Nevertheless, the augmentation effect in improving the final result was significant that was not covered in the previous studies.

7 Conclusion

In this study, a supervised deep learning based approach is employed to address mass lesion classification from mammographic data. For this aim, we have proposed and compared various ways of train data augmentation for training the AlexNet architecture. In the first experiment, an extended augmentation scheme is applied on the raw extracted annotated mass and the network learns directly from this training data. In the second experiment, responses of a suggested filter bank are also fed to the network. Finally, in the third experiment, a texton-based approach is utilised to model pre-detected mass abnormalities in mammograms in the form of particular RoI-texton-models to explain salient features contained in each input image. Subsequently, these processed RoI-texton-models are fed to the CNN architecture along with the other augmented train samples. We evaluated the results on the DDSM dataset and obtained the accuracy of 87% which is comparable to the current approach outcomes and can be considered in real world settings.

Acknowledgments. The authors would like to gratefully acknowledge Sandy Spence and Alun Jones for their support and maintenance of the GPU and the systems used for this research.

References

[1] Breasr Cancer Biopsy (2015), http://www.breastcancer.org/symptoms/testing/types/biopsy
[2] National Health Service- Breast screening: professional guidance (31 August 2016), https://www.gov.uk/government/collections/breast-screening-professional-guidance
[3] Arevalo, J., González, F.A., Ramos-Pollán, R., Oliveira, J.L., Lopez, M.A.G.: Representation learning for mammography mass lesion classification with convolutional neural networks. Computer Methods and Programs in Biomedicine 127, 248–257 (2016)
[4] Buciu, I., Gacsadi, A.: Directional features for automatic tumor classification of mammogram images. Biomedical Signal Processing and Control 6(4), 370–378 (2011)
[5] Carneiro, G., Nascimento, J., Bradley, A.P.: Unregistered multiview mammogram analysis with pre-trained deep learning models. In: International Conference onMedical Image Computing and Computer-Assisted Intervention. pp. 652–660. Springer (2015)
[6] Cheng, S.C., Huang, Y.M.: A novel approach to diagnose diabetes based on the fractal characteristics of retinal images. IEEE Transactions on Information Technology in Biomedicine 7(3), 163–170 (2003)
[7] Deng, J., Dong, W., Socher, R., Li, L.J., Li, K., Fei-Fei, L.: ImageNet: A large-scale hierarchical image database. In: IEEE Conference on Computer Vision and Pattern Recognition, 2009. CVPR'09. pp. 248–255 (2009)
[8] Dhungel, N., Carneiro, G., Bradley, A.P.: Automated mass detection in mammograms using cascaded deep learning and random forests. In: IEEE International Conference on Digital Image Computing: Techniques and Applications (DICTA). pp. 1–8 (2015)
[9] Fonseca, P., Mendoza, J., Wainer, J., Ferrer, J., Pinto, J., Guerrero, J., Castaneda, B.: Automatic breast density classification using a convolutional neural network architecture search procedure. In: SPIE Medical Imaging. vol. 9414 (2015)
[10] Greenspan, H., van Ginneken, B., Summers, R.M.: Guest editorial deep learning in medical imaging: Overview and future promise of an exciting new technique. IEEE Transactions on Medical Imaging 35(5), 1153–1159 (2016)
[11] Heath, M., Bowyer, K., Kopans, D., Moore, R., Kegelmeyer, W.P.: The digital database for screening mammography. In: In Proceedings of the 5th International Workshop on Digital Mammography. pp. 212–218. Medical Physics Publishing (2001)
[12] Huynh, B.Q., Li, H., Giger, M.L.: Digital mammographic tumor classification using transfer learning from deep convolutional neural networks. Journal of Medical Imaging 3(3), 034501 (2016)
[13] Jamieson, A.R., Drukker, K., Giger, M.L.: Breast image feature learning with adaptive deconvolutional networks. In: SPIE Medical Imaging. vol. 8315 (2012)
[14] Jia, Y., Shelhamer, E., Donahue, J., Karayev, S., Long, J., Girshick, R., Guadarrama, S., Darrell, T.: Caffe: Convolutional Architecture for Fast Feature Embedding. arXiv preprint arXiv:1408.5093 (2014)

[15] Jiao, Z., Gao, X., Wang, Y., Li, J.: A deep feature based framework for breast masses classification. Neurocomputing 197, 221–231 (2016)
[16] Kallenberg, M., Petersen, K., Nielsen, M., Ng, A.Y., Diao, P., Igel, C., Vachon, C.M., Holland, K., Winkel, R.R., Karssemeijer, N.: Unsupervised deep learning applied to breast density segmentation and mammographic risk scoring. IEEE Transactions on Medical Imaging 35(5), 1322–1331 (2016)
[17] Kooi, T., Gubern-Merida, A., Mordang, J.J., Mann, R., Pijnappel, R., Schuur, K., den Heeten, A., Karssemeijer, N.: A comparison between a deep convolutional neural network and radiologists for classifying regions of interest in mammography. In: International Workshop on Digital Mammography. vol. 9699, pp. 51–56. Springer (2016)
[18] Krizhevsky, A., Sutskever, I., Hinton, G.E.: ImageNet classification with deep convolutional neural networks. In: Advances in Neural Information Processing Systems. pp. 1097–1105 (2012)
[19] Lévy, D., Jain, A.: Breast mass classification from mammograms using deep convolutional neural networks. 30th Conference on Neural Information Processing Systems (NIPS), Barcelona, Spain, arXiv preprint arXiv:1612.00542 (2016)
[20] Oliver, A., Freixenet, J., Marti, J., Pérez, E., Pont, J., Denton, E.R., Zwiggelaar, R.: A review of automatic mass detection and segmentation in mammographic images. Medical Image Analysis 14(2), 87–110 (2010)
[21] Petersen, K., Chernoff, K., Nielsen, M., Ng, A.Y.: Breast density scoring with multiscale denoising autoencoders. In: in: STMI workshop at MICCAI. vol. 2012 (2012)
[22] Pinto, N., Doukhan, D., DiCarlo, J.J., Cox, D.D.: A high-throughput screening approach to discovering good forms of biologically inspired visual representation. PLoS computational biology 5(11), e1000579 (2009)
[23] Ranzato, M., Poultney, C., Chopra, S., Cun, Y.L.: Efficient learning of sparse representations with an energy-based model. In: Advances in Neural Information Processing Systems. pp. 1137–1144 (2006)
[24] Russakovsky, O., Deng, J., Su, H., Krause, J., Satheesh, S., Ma, S., Huang, Z., Karpathy, A., Khosla, A., Bernstein, M., BergLi, A.C., Fei-Fei, L.: Imagenet large scale visual recognition challenge. International Journal of Computer Vision 115(3), 211–252 (2015)
[25] Serifovic-Trbalic, A., Trbalic, A., Demirovic, D., Prljaca, N., Cattin, P.: Classification of benign and malignant masses in breast mammograms. In: 37th International Convention on Information and Communication Technology, Electronics and Microelectronics (MIPRO). pp. 228–233. IEEE (2014)
[26] Stewart, B., Wild, C.P., International Agency for Research on Cancer, W.: World Cancer Report (2014)
[27] Tajbakhsh, N., Shin, J.Y., Gurudu, S.R., Hurst, R.T., Kendall, C.B., Gotway, M.B., Liang, J.: Convolutional neural networks for medical image analysis: Full training or fine tuning? IEEE transactions on medical imaging 35(5), 1299–1312 (2016)
[28] Vaidehi, K., Subashini, T.: Automatic characterization of benign and malignant masses in mammography. Procedia Computer Science 46, 1762–1769 (2015)
[29] Varma, M., Zisserman, A.: Texture classification: Are filter banks necessary? In: IEEE Conference on Computer Vision and Pattern Recognition. vol. 2, pp. II–691. IEEE (2003)
[30] Varma, M., Zisserman, A.: A statistical approach to texture classification from single images. International Journal of Computer Vision 62(1-2), 61–81 (2005)